Bending and Buckling Analysis of a Nth-Order Shear Deformation Nanoplate using Modified Couple Stress Theory

Majid Eskandari Shahraki
Department of Aerospace Engineering,
Ferdowsi University of Mashhad, Mashhad, Iran
E-mail: mjdeskandari@gmail.com

Mahmoud Shariati
Department of Mechanical Engineering,
Ferdowsi University of Mashhad, Mashhad, Iran
E-mail: mshariati44@um.ac.ir

Naser Asiaban*
Department of Mechanical Engineering,
Ferdowsi University of Mashhad, Mashhad, Iran
E-mail: naser.asiaban@mail.um.ac.ir
*Corresponding author

Received: 15 November 2020, Revised: 16 February 2021, Accepted: 23 February 2021

Abstract: In this paper a Nth order nanoplate model is developed for the bending and buckling analysis of a graphene nanoplate based on a modified couple stress theory. The strain energy, external work and buckling equations are solved. Also using Hamilton' principle, main and auxiliary equations of nano plate are obtained. The bending rates and dimensionless bending values under uniform surface traction and sinusoidal load, the dimensionless critical force under a uniaxial surface force in x direction are all obtained for various plate's dimensional ratios and material length scale to thickness ratios. The governing equations are numerically solved. The effect of material length scale, length, width and thickness of the nanoplate on the bending and buckling ratios are investigated and the results are presented and discussed in details.

Keywords: Buckling, Bending, Modified Couple Stress Theory, Navier's Solution, Nth-Order Nanoplate

How to cite this paper: Majid Eskandari Shahraki, Mahmoud Shariati, and Naser Asiaban, "Bending and Buckling Analysis of a Nth-Order Shear Deformation Nanoplate using Modified Couple Stress Theory" , Int J of Advanced Design and Manufacturing Technology, Vol. 14/No. 4, 2021, pp. 27–36.
DOI: 10.30495/admt.2021.1915086.1229

Biographical notes: Majid Eskandari Shahraki is currently a PhD student at Ferdowsi University of Mashhad, Iran. He received his MSc in Mechanical Engineering from IAU Univesity, Khomeini Shahr branch, Isfahan, Iran in 2014. His main research interests is nanomechanics. **Mohmoud Shariati** is a Professor of Mechanical Engineering at Ferdowsi University of Mashhad, Iran. He received his PhD in Mechanical Engineering from Tarbiat Modarres Univesity, Tehran, Iran in 1999. His current research interest includes nanomechanics, experimental mechanics, fatigue and fracture Iran**. Naser Asiaban** is currently a PhD student at Ferdowsi University of Mashhad, Iran. He received his MSc in Mechanical Engineering from Babol Noshirvani University of Technology (BNUT), Babol, Iran in 2016. His field of research are simulation of liquid composite molding (LCM) processes and renewable energies.

1 INTRODUCTION

Performing experiments in the atomic and molecular scales are the safest approach for the study of materials in small-scale. In this method, the nanostructures are studied in real dimensions. In this method in order to determine the mechanical properties of nanostructures, the Atomic Force Microscopy (AFM) applies different mechanical loads on nanoplates and measures the plate responses. The difficulties of controlling the test conditions at this scale, high economic costs and time-consuming processes are some setbacks of this method. Therefore, it is only used to validate other simple and low-cost methods.

Atomic simulation is another approach for studying small-scale structures. In this method, the behaviors of atoms and molecules are examined by considering the intermolecular and interatomic effects on their motions, which eventually involves the total deformation of the body. In the case of large deformations and multi atomic scales, the computational costs of this approach become unbearable, so it is only used for small deformation problems.

Given the limitations of the aforementioned methods, researchers have been looking for simpler solutions for studying nanostructures. Modeling small-scale structures using continuum mechanics is another approach for this problem. There are a variety of size-dependent continuum theories that consider size effects, some of these theories are; micromorphic theory, microstructural theory, micropolar theory, Kurt's theory, non-local theory, modified couple stress theory and strain gradient elasticity. All of which are the developed notion of classical field theories, which includes size effects. Daghigh et al, studied the nonlocal bending and buckling of agglomerated CNT-Reinforced composite nanoplates. They investigated the effect of the parameters, such are degree of agglomeration, nonlocal material scale parameter, temperature, foundation properties, volume fraction of CNTs, and length-to-thickness aspect ratio for the plate [1].

Daikh et al, studied A novel nonlocal strain gradient Quasi-3D bending analysis of sigmoid functionally graded sandwich nanoplates. They investigated the effect of the elastic foundation models, sigmoidal distribution index constant, configuration of sandwich plate, material and length nanoscales, boundary conditions on the static deflection [2]. Ruocco et al, studied the buckling analysis of elastic–plastic nanoplates resting on a Winkler–Pasternak foundation based on nonlocal third-order plate theory. They investigated the effect of geometrical, constitutive, and nonlocal parameters on the critical behavior of plates with different boundary conditions [3].

Banh-Thien et al, studied the buckling analysis of non-uniform thickness nanoplates in an elastic medium using the isogeometric analysis. They discretized the governing equation into algebraic equations and solved by using IGA procedure to determine the critical buckling load. By using the non-uniform rational B-splines, IGA easily satisfies the required continuity of the partial differential equations in buckling analysis [4]. In this paper, a Nth order nanoplate model is developed for the bending and buckling analysis of a graphene nanoplate based on a modified couple stress theory and the results are presented with new figures and tables.

2 MODIFIED COUPLE STRESS THEORY

In 2002, Yang et al. [5] proposed a modified couple stress model by modifying the theory proposed by Toppin [6], Mindlin and Thursten [7], Quitter [8] and Mindlin [9] in 1964. The modified couple stress theory consists of only one material length scale parameter for projection of the size effect, whereas the classical couple stress theory needs two material length scale parameters. In the modified theory, the strain energy density in the three-dimensional vertical coordinates for a body bounded by the volume V and the area Ω [10], is expressed as the follows:

$$U = \frac{1}{2}\int_V \left(\sigma_{ij}\varepsilon_{ij} + m_{ij}\chi_{ij}\right)dV \quad i, j = 1,2,3 \qquad (1)$$

$$\varepsilon_{ij} = \frac{1}{2}(u_{i,j} + u_{j,i}) \qquad (2)$$

$$\chi_{ij} = \frac{1}{2}\left(\theta_{i,j} + \theta_{j,i}\right) \qquad (3)$$

χ_{ij} and ε_{ij} are the symmetric parts of the curvature and strain tensors, and θ_i and u_i are the displacement and the rotational vectors, respectively:

$$\theta = \frac{1}{2}\, Curl\, \boldsymbol{u} \qquad (4)$$

σ_{ij}, the stress tensor, and $m_{i,j}$, the deviatory part of the couple stress tensor, are defined as:

$$\sigma_{ij} = \lambda\varepsilon_{kk}\delta_{ij} + 2\mu\varepsilon_{ij} \qquad (5)$$

$$m_{i,j} = 2\mu\, l^2\chi_{ij} \qquad (6)$$

Where, λ and μ are the lame constants, δ_{ij} is the Kronecker delta and l is the material length scale parameter. From Equations (3) and (6), it can be seen that χ_{ij} and m_{ij} are symmetric.

3 NTH-ORDER PLATE MODEL

The displacement equations for the nth-order plate are described as follows:

$$u_1(x,y,z) = z\varphi_x(x,y) - \frac{1}{n}\left(\frac{2}{h}\right)^{n-1} z^n\left(\frac{\partial w(x,y)}{\partial x} + \varphi_x(x,y)\right)$$

$$u_2(x,y,x) = z\varphi_y(x,y) - \frac{1}{n}\left(\frac{2}{h}\right)^{n-1} z^n\left(\frac{\partial w(x,y)}{\partial y} + \varphi_y(x,y)\right), \; n = 3, 5, 7, 9, \ldots \quad (7)$$

$$u_3(x,y,z) = w(x,y)$$

Where, φ_x and φ_y are the rotations of the normal vector around the x and y axis, respectively, and w is the midpoint displacement of the plate in the z-axis direction. The strain and stress tensors, the symmetric part of the curvature tensor, and the rotational vector for the nth-order plate are obtained as follows:

$$\mathcal{E}_{xx} = z\frac{\partial\varphi_x}{\partial x} - \frac{1}{n}\left(\frac{2}{h}\right)^{n-1} z^n\left(\frac{\partial^2 w}{\partial x^2} + \frac{\partial\varphi_x}{\partial x}\right) \quad (8)$$

$$\mathcal{E}_{yy} = z\frac{\partial\varphi_y}{\partial y} - \frac{1}{n}\left(\frac{2}{h}\right)^{n-1} z^n\left(\frac{\partial^2 w}{\partial y^2} + \frac{\partial\varphi_y}{\partial y}\right) \quad (9)$$

$$\mathcal{E}_{zz} = 0 \quad (10)$$

$$\mathcal{E}_{xy} = \mathcal{E}_{yx} = \frac{1}{2}z\left(\frac{\partial\varphi_x}{\partial y} + \frac{\partial\varphi_y}{\partial x}\right) - \frac{1}{2n}\left(\frac{2}{h}\right)^{n-1} z^n\left(\frac{\partial\varphi_x}{\partial y} + \frac{\partial\varphi_y}{\partial x} + 2\frac{\partial^2 w}{\partial x\partial y}\right) \quad (11)$$

$$\mathcal{E}_{xz} = \mathcal{E}_{zx} = \frac{1}{2}\left(1 - \left(\frac{2z}{h}\right)^{n-1}\right)\left(\frac{\partial w}{\partial x} + \varphi_x\right) \quad (12)$$

$$\mathcal{E}_{yz} = \mathcal{E}_{zy} = \frac{1}{2}\left(1 - \left(\frac{2z}{h}\right)^{n-1}\right)\left(\frac{\partial w}{\partial y} + \varphi_y\right) \quad (13)$$

$$\theta_x = \frac{\partial w}{\partial y} - \frac{1}{2}\left(1 - \left(\frac{2z}{h}\right)^{n-1}\right)\left(\frac{\partial w}{\partial y} + \varphi_y\right) \quad (14)$$

$$\theta_y = -\frac{\partial w}{\partial x} + \frac{1}{2}\left(1 - \left(\frac{2z}{h}\right)^{n-1}\right)\left(\frac{\partial w}{\partial x} + \varphi_x\right) \quad (15)$$

$$\theta_z = \frac{1}{2}\left(z - \frac{1}{n}\left(\frac{2}{h}\right)^{n-1} z^n\right)\left(\frac{\partial\varphi_y}{\partial x} - \frac{\partial\varphi_x}{\partial y}\right) \quad (16)$$

$$x_{xx} = \frac{\partial^2 w}{\partial x\,\partial y} - \frac{1}{2}\left(1 - \left(\frac{2z}{h}\right)^{n-1}\right)\left(\frac{\partial^2 w}{\partial x\,\partial y} + \frac{\partial\varphi_y}{\partial x}\right) \quad (17)$$

$$x_{yy} = -\frac{\partial^2 w}{\partial x\partial y} + \frac{1}{2}\left(1 - \left(\frac{2z}{h}\right)^{n-1}\right)\left(\frac{\partial\varphi_x}{\partial y} + \frac{\partial^2 w}{\partial x\partial y}\right) \quad (18)$$

$$x_{zz} = \frac{1}{2}\left(1 - \left(\frac{2z}{h}\right)^{n-1}\right)\left(\frac{\partial\varphi_y}{\partial x} - \frac{\partial\varphi_x}{\partial y}\right) \quad (19)$$

$$x_{xy} = \frac{1}{2}\left(\frac{\partial^2 w}{\partial y^2} - \frac{\partial^2 w}{\partial x^2}\right) + \frac{1}{4}\left(1 - \left(\frac{2z}{h}\right)^{n-1}\right) * \left(\frac{\partial^2 w}{\partial x^2} + \frac{\partial\varphi_x}{\partial x} - \frac{\partial^2 w}{\partial y^2} - \frac{\partial\varphi_y}{\partial y}\right) \quad (20)$$

$$x_{xz} = \frac{1}{4}\left(z - \frac{1}{n}\left(\frac{2}{h}\right)^{n-1} z^n\right)\left(\frac{\partial^2\varphi_y}{\partial x^2} - \frac{\partial^2\varphi_x}{\partial y\,\partial x}\right) \frac{1}{4}\left(\left(\frac{2}{h} - \frac{2n}{h}\right)\left(\frac{2z}{h}\right)^{n-2}\right)\left(\frac{\partial w}{\partial y} + \varphi_y\right) \quad (21)$$

$$x_{yz} = \frac{1}{4}\left(\left(\frac{2}{h} - \frac{2n}{h}\right)\left(\frac{2z}{h}\right)^{n-2}\right)\left(\frac{\partial w}{\partial x} + \varphi_x\right) + \frac{1}{4}\left(z - \frac{1}{n}\left(\frac{2}{h}\right)^{n-1} z^n\right)\left(\frac{\partial^2\varphi_y}{\partial x\partial y} - \frac{\partial^2\varphi_x}{\partial y^2}\right) \quad (22)$$

$$\sigma_{xx} = (\lambda + 2\mu)\mathcal{E}_{xx} + \lambda\mathcal{E}_{yy} \quad (23)$$

$$\sigma_{yy} = \lambda\mathcal{E}_{xx} + (\lambda + 2\mu)\mathcal{E}_{yy} \quad (24)$$

$$\sigma_{zz} = \lambda(\mathcal{E}_{xx} + \mathcal{E}_{yy}) \quad (25)$$

$$\sigma_{yx} = \sigma_{xy} = 2\mu\,\mathcal{E}_{xy} \quad (26)$$

$$\sigma_{xz} = \sigma_{zx} = 2\mu\,\mathcal{E}_{xz} \quad (27)$$

$$\sigma_{yz} = \sigma_{zy} = 2\mu\,\mathcal{E}_{yz} \quad (28)$$

The variation of strain energy is expressed as follows:

$$\delta U = \int_V (\sigma_{xx}\,\delta\,\mathcal{E}_{xx} + \sigma_{yy}\,\delta\mathcal{E}_{yy} + 2\sigma_{xy}\,\delta\,\mathcal{E}_{xy} + \sigma_{xz}\,\delta\,\mathcal{E}_{xz} + 2\sigma_{yz}\,\delta\,\mathcal{E}_{yz} + m_{xx}\,\delta\,x_{xx} + m_{yy}\,\delta x_{yy} + m_{zz}\,\delta x_{zz} + 2m_{xy}\,\delta x_{xy} + 2m_{xz}\,\delta x_{xz} + 2m_{yz}\,\delta\,x_{yz})dV \quad (29)$$

For the sake of simplification, the coefficient of each variable in the above equation is named from F_1 to F_{15} and this equation can be rewritten as shown below:

$$U = \int_V (F_1\delta w_{,xx} + F_2\,\delta w_{,yy} + F_3\,\delta w_{,xy} + F_4\delta\,w_{,x} + F_5\,\delta\,w_{,y} + F_6\,\delta\,\varphi_{x,yy} + F_7\delta\,\varphi_{y,xx} + F_8\,\delta\,\varphi_{x,y} + F_9\,\delta\varphi_{x,yx} + F_{10}\,\delta\,\varphi_{x,x} + F_{12}\delta\varphi_{x,y} + F_{13}\,\delta\,\varphi_{y,x} + F_{14}\,\delta\varphi_x + F_{15}\,\delta\varphi_y)dV \quad (30)$$

Where, F_1 to F_{15} are calculated as shown:

$$F_1 = \frac{\partial^2 w}{\partial x^2}[(\lambda + 2\mu)(A_3 - A_1A_2) + \frac{1}{2}\mu l^2(1 + A_4) - \frac{1}{4}\mu l^2(1 + A_4)(1 - A_4)] + \frac{\partial^2 w}{\partial y^2}[(A_3 - A_1A_2) - \frac{1}{2}\mu l^2(1 + A_4) + \frac{1}{4}\mu l^2(1 - A_4)(1 + A_4)] + \frac{\partial\varphi_y}{\partial y}[-\lambda(A_2A_1) - \frac{1}{4}\mu l^2(1 - A_4)(1 + A_4)] \quad (31)$$

$$F_2 = \frac{\partial^2 w}{\partial y^2}[(\lambda+2\mu)(A_3 - A_1A_2) + \frac{1}{2}\mu l^2(1+A_4) - \frac{1}{4}\mu l^2] + \frac{\partial^2 w}{\partial x^2}[\lambda(A_3 - A_1A_2) - \frac{1}{2}\mu l^2(1+A_4) + \frac{1}{4}\mu l^2(1 - A_4)(1+A_4)] + \frac{\partial \varphi_y}{\partial y}\left[-(\lambda+2\mu)(A_2A_1) - \frac{1}{4}\mu l^2(1 - A_4)(1+A_4)\right] + \frac{\partial \varphi_x}{\partial x}\left[-\lambda(A_2A_1) - \frac{1}{4}\mu l^2(1 - A_4)(1+A_4)\right] \quad (32)$$

$$F_3 = \frac{\partial^2 w}{\partial x\,\partial y}\left[4\mu\, {A_2}^2 + \mu l^2(1+A_4)^2\right] + \frac{\partial \varphi_x}{\partial y}\left[-2\mu A_2A_1 - \frac{1}{2}\mu l^2(1 - A_4)(1+A_4)\right] + \left[-2\mu A_2A_1 - \frac{1}{2}\mu l^2(1 - A_4)(1+A_4)\right] \quad (33)$$

$$F_4 = \left(\frac{\partial w}{\partial x} + \varphi_x\right)\left[\mu(1 - A_4)^2 + \frac{1}{4}\mu l^2 {A_5}^2\right] + \left(\frac{\partial^2 \varphi_y}{\partial x \partial y} - \frac{\partial^2 \varphi_x}{\partial y^2}\right)\left[\frac{1}{4}\mu l^2 A_5A_1\right] \quad (34)$$

$$F_5 = \left(\frac{\partial w}{\partial y} + \varphi_y\right)\left[\mu(1 - A_4)^2 + \frac{1}{4}\mu l^2 {A_5}^2\right] + \left(\frac{\partial^2 \varphi_x}{\partial x \partial y} - \frac{\partial^2 \varphi_y}{\partial x^2}\right)\left[\frac{1}{4}\mu l^2 A_5A_1\right] \quad (35)$$

$$F_6 = F_8 = \left(\frac{\partial w}{\partial x} + \varphi_x\right)\left[\frac{1}{4}\mu l^2 A_5A_1\right] + \left(\frac{\partial^2 \varphi_y}{\partial x \partial y} - \frac{\partial^2 \varphi_x}{\partial y^2}\right)\left[\frac{1}{4}\mu l^2 {A_1}^2\right] \quad (36)$$

$$F_7 = F_9 = \left(\frac{\partial w}{\partial y} + \varphi_y\right)\left[-\frac{1}{4}\mu l^2 A_5A_1\right] + \left(\frac{\partial^2 \varphi_y}{\partial x^2} - \frac{\partial^2 \varphi_x}{\partial x \partial y}\right)\left[\frac{1}{4}\mu l^2 {A_1}^2\right] \quad (37)$$

$$F_{10} = \frac{\partial^2 w}{\partial x^2}\left[(\lambda+2\mu)\left({A_1}^2 - zA_1\right) - \frac{1}{4}\mu l^2(1 - A_4)(1+A_4)\right] + \frac{\partial^2 w}{\partial y^2}\left[\lambda A_1(-z+A_1) + \frac{1}{4}\mu l^2(1 - A_4)(1+A_4)\right] + \frac{\partial \varphi_x}{\partial x}\left[(\lambda+2\mu){A_1}^2 + \frac{1}{4}\mu l^2(1 - A_4)^2\right] + \frac{\partial \varphi_y}{\partial y}\left[\lambda {A_1}^2 - \frac{1}{4}\mu l^2(1 - A_4)^2\right] \quad (38)$$

$$F_{11} = \frac{\partial^2 w}{\partial y^2}\left[(\lambda+2\mu)\left({A_1}^2 - zA_1\right) - \frac{1}{4}\mu l^2(1 - A_4)(1+A_4)\right] + \frac{\partial^2 w}{\partial x^2}\left[\lambda A_1(-z+A_1) + \frac{1}{4}\mu l^2(1 - A_4)(1+A_4)\right] + \frac{\partial \varphi_y}{\partial y}\left[(\lambda+2\mu){A_1}^2 + \frac{1}{4}\mu l^2(1 - A_4)^2\right] + \frac{\partial \varphi_x}{\partial x}\left[\lambda {A_1}^2 - \frac{1}{4}\mu l^2(1 - A_4)^2\right] \quad (39)$$

$$F_{12} = \frac{\partial^2 w}{\partial x\,\partial y}\left[-2\mu A_2A_1 - \frac{1}{2}\mu l^2(1 - A_4)(1+A_4)\right] + \frac{\partial \varphi_x}{\partial y}\left[\mu {A_1}^2 + \mu l^2(1 - A_4)^2\right] + \frac{\partial \varphi_y}{\partial x}\left[\mu {A_1}^2 - \frac{1}{2}\mu l^2(1 - A_4)^2\right] \quad (40)$$

$$F_{13} = \frac{\partial^2 w}{\partial x\,\partial y}\left[-2\mu A_2A_1 - \frac{1}{2}\mu l^2(1 - A_4)(1+A_4)\right] + \frac{\partial \varphi_x}{\partial y}\left[\mu {A_1}^2 - \frac{1}{2}\mu l^2(1 - A_4)^2\right] + \frac{\partial \varphi_y}{\partial x}\left[\mu {A_1}^2 + \mu l^2(1 - A_4)^2\right] \quad (41)$$

$$F_{14} = \left(\frac{\partial w}{\partial x} + \varphi_x\right)\left[\mu(1 - A_4)^2 + \frac{1}{4}\mu l^2 {A_5}^2\right] + \left(\frac{\partial^2 \varphi_y}{\partial x \partial y} - \frac{\partial^2 \varphi_x}{\partial y^2}\right)\left[\frac{1}{4}\mu l^2 A_5A_1\right] \quad (42)$$

$$F_{15} = \left(\frac{\partial w}{\partial y} + \varphi_y\right)\left[\mu(1 - A_4)^2 + \frac{1}{4}\mu l^2 {A_5}^2\right] + \left(\frac{\partial^2 \varphi_x}{\partial x \partial y} - \frac{\partial^2 \varphi_y}{\partial x^2}\right)\left[\frac{1}{4}\mu l^2 A_5A_1\right] \quad (43)$$

In which we have:

$$A_1 = z - \frac{1}{n}\left(\frac{2}{h}\right)^{n-1} z^n \quad (44)$$

$$A_2 = \frac{1}{n}\left(\frac{2}{h}\right)^{n-1} z^n \quad (45)$$

$$A_3 = \frac{1}{n}\left(\frac{2}{h}\right)^{n-1} z^{n+1} \quad (46)$$

$$A_4 = \left(\frac{2z}{h}\right)^{n-1} \quad (47)$$

$$A_5 = \left(\frac{2}{h} - \frac{2n}{h}\right)\left(\frac{2z}{h}\right)^{n-2} \quad (48)$$

$$A_6 = \frac{1}{n}\left(\frac{2}{h}\right)^{n-1} \quad (49)$$

$$A_7 = \mu\left(\frac{2}{h}\right)^{n-1} I_{n-1} \quad (50)$$

$$A_8 = \mu\left(\frac{2}{h}\right)^{2n-2} I_{2n-2} \quad (51)$$

$$A_9 = (\lambda+2\mu)\left(\frac{1}{n}\left(\frac{2}{h}\right)^{n-1}\right)^2 I_{2n} \quad (52)$$

$$A_{10} = (\lambda+2\mu)\frac{1}{n}\left(\frac{2}{h}\right)^{n-1} I_{n+1} \quad (53)$$

$$A_{11} = \frac{1}{4}\mu\, l^2\left(\frac{1}{n}\left(\frac{2}{h}\right)^{n-1}\right)^2 (n^2-n)^2 I_{2n-4} \quad (54)$$

$$A_{12} = \frac{1}{4}\mu\, l^2 h \quad (55)$$

$$I_i = \int_{-\frac{h}{2}}^{\frac{h}{2}} Z^i\, dz \quad (56)$$

$$(i = 0, 1, 2, n-1, n, n+1, 2n-4, 2n-2, 2n)$$

4 THE BUCKLING FORCE

For a rectangular plate with length a, width b and thickness h, under the axial forces (P_{xy}, P_y, P_x), the buckling force is obtained as shown in equation (57) [11-12]:

$$P_x \frac{\partial^2 w}{\partial x^2} + 2P_{xy} \frac{\partial^2 w}{\partial x \partial y} + P_y \frac{\partial^2 w}{\partial y^2} = q(x,y) \quad (57)$$

Where, P_x is the Axial force along the x axis, P_y is the Axial force along the y axis, P_{xy} is the shear force in the xy plane, and q (x, y) is the out-of-plane force.

5 VIRTUAL WORK OF EXTERNAL FORCES

In these kind of problems, the virtual work of three kinds of external forces are included in the solutions, if the middle-plane and the middle-perimeter of the plate are shown as Ω and Γ respectively, these virtual works are [13]:

1. The virtual work done by the body forces, which is applied on the volume V= Ω× (- h⁄2, h⁄2).
2. The virtual work done by the surface tractions at the upper and lower surfaces (Ω).
3. The virtual work done by the shear tractions on the lateral surfaces, S= Γ× (- h⁄2, h⁄2).

If (f_x, f_y, f_z) are the body forces, (c_x, c_y, c_z) are the body couples, (q_x, q_y, q_z) are the forces acting on the Ω plane, (t_x, t_y, t_z) are the Cauchy's tractions and (S_x, S_y, S_z) are surface couples, the variations of the virtual work is expressed as:

$$\delta w = -\Big[\int_{\Omega} (f_x \delta u + f_y \delta V + f_z \delta w + q_x \delta u + q_y \delta V + q_z \delta w + c_x \delta\theta_x + c_y\, \delta\theta_y + c_z \delta\theta_z)\, dx\, dy + \int_{\Gamma} (t_x \delta u + t_y \delta V + t_z \delta w + s_x \theta_x + s_y \delta\theta_y + s_z \delta) \quad (58)$$

Given that in this study, only the external force q_z was applied, virtual work becomes:

$$\delta w = \int_0^a \int_0^b q(x,y) \delta w(x,y) dx\, dy \quad (59)$$

Finally using the Hamilton's principle, it can be said that [14]:

$$\delta(U - w) = 0 \quad (60)$$

6 THE FINAL GOVERNING EQUATIONS OF THE PLATE AFTER APPLYING THE BUCKLING AND EXTERNAL FORCES

Using Hamilton's principle, equation (60), and the equations from (57) to (59), the governing equations of the plate including the buckling and external forces are obtained as follows:

$$\left[\int_{-h/2}^{h/2} \left(\frac{\partial^2 F_1}{\partial x^2} - \frac{\partial F_4}{\partial x} + \frac{\partial^2 F_2}{\partial y^2} + \frac{\partial^2 F_3}{\partial x \partial y} - \frac{\partial F_5}{\partial y}\right) dz\right] + P_x \frac{\partial^2 w}{\partial x^2} + 2P_{xy} \frac{\partial^2 w}{\partial x \partial y} + P_y \frac{\partial^2 w}{\partial y^2} = q(x,y) \quad (61)$$

$$\int_{-h/2}^{h/2} \left(\frac{\partial^2 F_6}{\partial y^2} + \frac{\partial^2 F_9}{\partial x \partial y} - \frac{\partial F_{12}}{\partial y} - \frac{\partial F_{10}}{\partial x} + F_{14}\right) dz = 0 \quad (62)$$

$$\int_{-h/2}^{h/2} \left(\frac{\partial^2 F_7}{\partial x^2} - \frac{\partial F_{13}}{\partial x} + \frac{\partial^2 F_8}{\partial x \partial y} - \frac{\partial F_{11}}{\partial y} + F_{15}\right) dz = 0 \quad (63)$$

7 OBTAINING THE GENERAL GOVERNING EQUATION OF THE MINDLIN'S PLATE (INCLUDING BUCKLING AND BENDING)

Considering the following constants:

$$B_1 = 2A_{12} + l^2 A_7 + \tfrac{1}{2} l^2 A_8 + 2A_9 \quad (64)$$

$$B_2 = \frac{1}{2} B_1 = A_{12} + A_9 + \tfrac{1}{2} l^2 A_7 + \tfrac{1}{4} l^2 A_8 \quad (65)$$

$$B_3 = -\mu h + 2A_7 - A_8 - A_{11} \quad (66)$$

$$B_4 = A_9 - A_{10} + \tfrac{1}{4} l^2 A_8 - A_{12} \quad (67)$$

$$B_5 = 3A_{12} - \tfrac{3}{2} l^2 A_7 + \tfrac{3}{4} l^2 A_8 - (\lambda + \mu) I_2 + 2(\lambda + \mu) A_6\, I_{n+1} - (\lambda + \mu) {A_6}^2 I_{2n} \quad (68)$$

$$B_6 = -\mu I_2 + 2\mu A_6\, I_{n+1} - \mu {A_6}^2 I_{2n} - 4A_{12} + 2l^2 A_7 - l^2 A_8 \quad (69)$$

$$B_7 = \tfrac{1}{4} \mu l^2 I_2 - \tfrac{1}{2} \mu l^2 A_6 I_{n+1} + \tfrac{1}{4} \mu l^2 {A_6}^2 I_{2n} \quad (70)$$

$$B_8 = -(\lambda + 2\mu) I_2 + 2A_{10} - A_9 - A_{12} + \tfrac{1}{2} l^2 A_7 - \tfrac{1}{4} l^2 A_8 \quad (71)$$

$$B_9 = \tfrac{5}{4} l^2 A_8 - \tfrac{1}{2} \mu l^2 n {A_6}^2 I_{2n-2} - l^2 A_7 - \tfrac{1}{2} l^2 n A_7 + 3A_{12} - (\lambda + \mu) I_2 - (\lambda + \mu) {A_6}^2 I_{2n} + 2(\lambda + \mu) A_6 I_{n+1} \quad (72)$$

$$B_{10} = \tfrac{3}{2} l^2 A_7 + \tfrac{1}{2} l^2 n A_7 - \tfrac{3}{2} l^2 A_8 + \tfrac{1}{2} \mu l^2 n {A_6}^2 I_{2n-2} - \mu I_2 - \mu {A_6}^2 I_{2n} + 2\mu A_6 I_{n+1} - 4A_{12} \quad (73)$$

The general governing equation of the Mindlin's plate will become:

$$B_1\frac{\partial^4 w}{\partial x^2\,\partial y^2}+B_2\frac{\partial^4 w}{\partial x^4}+B_2\frac{\partial^4 w}{\partial y^4}+B_3\frac{\partial^2 w}{\partial x^2}+B_3\frac{\partial^2 w}{\partial y^2}+B_4\frac{\partial^3 \varphi_x}{\partial x^3}+B_4\frac{\partial^3 \varphi_x}{\partial x\,\partial y^2}+B_4\frac{\partial^3 \varphi_y}{\partial y\,\partial x^2}+B_3\frac{\partial \varphi_x}{\partial x}+B_3\frac{\partial \varphi_y}{\partial y}+B_4\frac{\partial^3 \varphi_y}{\partial y^3}+P_x\frac{\partial^2 w}{\partial x^2}+2P_{xy}\frac{\partial^2 w}{\partial x\partial y}+P_y\frac{\partial^2 w}{\partial y^2}=q(x,y) \quad (74)$$

$$-B_4\frac{\partial^3 w}{\partial x\,\partial y^2}+B_5\frac{\partial^2 \varphi_y}{\partial y\,\partial x}+B_6\frac{\partial^2 \varphi_x}{\partial y^2}+B_7\frac{\partial^4 \varphi_y}{\partial x\,\partial y^3}-B_7\frac{\partial^4 \varphi_x}{\partial y^4}+B_7\frac{\partial^4 \varphi_y}{\partial y\,\partial x^3}-B_7\frac{\partial^4 \varphi_x}{\partial y^2\,\partial x^2}-B_3\frac{\partial w}{\partial x}-B_3\varphi_x-B_4\frac{\partial^3 w}{\partial x^3}+B_8\frac{\partial^2 \varphi_x}{\partial x^2}=0 \quad (75)$$

$$-B_4\frac{\partial^3 w}{\partial y\,\partial x^2}+B_9\frac{\partial^2 \varphi_x}{\partial y\,\partial x}+B_{10}\frac{\partial^2 \varphi_y}{\partial x^2}+B_7\frac{\partial^4 \varphi_y}{\partial x^4}+B_7\frac{\partial^4 \varphi_y}{\partial x^2\,\partial y^2}-B_7\frac{\partial^4 \varphi_x}{\partial y\,\partial x^3}-B_7\frac{\partial^4 \varphi_x}{\partial x\,\partial y^3}-B_4\frac{\partial^3 w}{\partial y^3}-B_3\frac{\partial w}{\partial y}-B_3\varphi_y+B_8\frac{\partial^2 \varphi_y}{\partial y^2}=0 \quad (76)$$

8 SOLUTION OF THE GOVERNING EQUATIONS USING NAVIER'S METHOD

The Navier's solution is applicable to the rectangular plates which have simply supported boundary conditions on all edges. Since the boundary conditions are spontaneously satisfied in this method, the unknown functions of the plate's mid-plane were assumed to be double trigonometric series [11], [13]:

$$W(x,y,t)=\sum_{m=1}^{\infty}\sum_{n=1}^{\infty}W_{mn}\sin\alpha x\sin\beta y\,e^{i\omega t} \quad (77)$$

$$\varphi_x(x,y,t)=\sum_{m=1}^{\infty}\sum_{n=1}^{\infty}X_{mn}\cos\alpha x\sin\beta y\,e^{i\omega t} \quad (78)$$

$$\varphi_y(x,y,t)=\sum_{m=1}^{\infty}\sum_{n=1}^{\infty}y_{mn}\sin\alpha x\cos\beta y\,e^{i\omega t} \quad (79)$$

The force can also be calculated from the following relations:

$$q=\sum_{m=1}^{\infty}\sum_{n=1}^{\infty}Q_{mn}\sin\alpha x\sin\beta y\,e^{i\omega t} \quad (80)$$

$$Q_{mn}=\frac{4}{ab}\int_0^a\int_0^b q(x,y)\sin\alpha x\sin\beta y\,dx\,dy \quad (81)$$

$$Q_{mn}=\begin{cases}q_0 & ;\ For\ sinusoidal\ force\\ \frac{16q_0}{mn\pi^2} & ;For\ uniform\ force\\ \frac{4Q_0}{ab} & ;For\ point\ force\ in\ the\ plane\ center\end{cases} \quad (82)$$

Where:

$$\alpha=\frac{\pi m}{a}\ ,\ \beta=\frac{\pi n}{b}\ ,\ i=\sqrt{-1} \quad (83)$$

Simply-supported boundary conditions were also satisfied by the Navier's method according to the following equations:

$$\begin{matrix}x=0\\ ,\\ x=a\end{matrix}\begin{cases}w(0,y)=w(a,y)=\sum\sum w_{mn}\sin\frac{m\pi}{a}x\sin\frac{n\pi}{b}y=0\\ \varphi_y(0,y)=\varphi_y(a,y)=\sum\sum y_{mn}\sin\frac{m\pi}{a}x\cos\frac{n\pi}{b}y=0\end{cases} \quad (84)$$

$$\begin{matrix}y=0\\ ,\\ y=b\end{matrix}\begin{cases}w(x,0)=w(x,b)=\sum\sum w_{mn}\sin\frac{m\pi}{a}x\sin\frac{n\pi}{b}y=0\\ \varphi_x(x,0)=\varphi_x(x,b)=\sum\sum X_{mn}\cos\frac{m\pi}{a}x\sin\frac{n\pi}{b}y=0\end{cases} \quad (85)$$

9 THE GENERAL EQUATION MATRIX OF A MINDLIN'S PLANE

After solving the governing equations and naming the coefficient of each variable, we have:

$$M_1=B_1\alpha^2\beta^2+B_2\alpha^4+B_2\beta^4-B_3\alpha^2-B_3\beta^2-P_x\alpha^2-P_y\beta^2 \quad (86)$$

$$M_2=M_4=B_4\alpha^3+B_4\alpha\,\beta^2-B_3\alpha \quad (87)$$

$$M_3=M_7=B_4\beta^3+B_4\alpha^2\beta-B_3\beta \quad (88)$$

$$M_5=-B_7\beta^4-B_7\alpha^2\beta^2-B_6\beta^2-B_8\alpha^2-B_3 \quad (89)$$

$$M_6=B_7\alpha\beta^3+B_7\alpha^3\beta-B_5\alpha\beta \quad (90)$$

$$M_8=-B_7\alpha^3\beta-B_7\alpha\beta^3-B_9\alpha\beta \quad (91)$$

$$M_9=B_7\,\alpha^4+B_7\alpha^2\beta^2-B_{10}\alpha^2-B_8\beta^2-B_3 \quad (92)$$

Finally, the general equation matrix of the Mindlin's plate along with the auxiliary equations will be obtained as follows:

$$\begin{bmatrix}M_1 & M_2 & M_3\\ M_4 & M_5 & M_6\\ M_7 & M_8 & M_9\end{bmatrix}\begin{bmatrix}w_{mn}\\ X_{mn}\\ y_{mn}\end{bmatrix}=\begin{bmatrix}Q_{mn}\\ 0\\ 0\end{bmatrix} \quad (93)$$

Various materials such as epoxy, graphene, copper and so on can be considered as the plate's material. In this study, graphene is chosen as the plate's material. A single-layer graphene plate has the following properties [14]:

$$E=1.06TPa,\ \nu=0.25\ ,\ h=0.34nm,\ \rho=2250\,{}^{kg}/_{m^3}$$

Also, the relationship between E, μ and ν can be expressed as:

$$\lambda = \frac{\nu E}{(1+\nu)(1-2\nu)} \quad , \mu = \frac{E}{2(1+\nu)} \tag{94}$$

Where, μ and λ are the lame's coefficients and E is the Young's modulus [15]. The value of the distributed force was considered to be q = 1N/m^2.

10 RESULTS & DISCUSSIONS

Results were obtained using a computational program coded in the MATLAB software. The results have also been compared with the literature [16-18] and good agreements between results were observed. The plate's dimensional parameters are chosen as follows:

a: plate's length
b: plate's width
h: plate's thickness
l: material length scale parameter

Tables 1 and 2 show the Mindlin's nanoplate bending rate under uniform surface traction for different material length scale parameters to thickness (l/h) and length to width ratio (a/b). As can be seen, as the length scale parameter to thickness ratio increases, the bending ratio decreases but it increases due to the increase in the plate's length to width ratio.

Table 1 The Mindlin's nanoplate bending rate under sinusoidal load for different length to width and material length scale to thickness ratios (n=3, q=1e-18 N/nm^2, a/h=30)

	l/h			
a/b	0	0.5	1	2
1	10.7837	5.3783	2.1483	0.6315
1.5	20.7713	10.3671	4.1428	1.2179
2	28.0010	13.9789	5.5868	1.6426

Table 2 The Mindlin's nanoplate bending rate under sinusoidal load for different length to width and material length scale to thickness ratios (n=5, q=1e-18 N/nm^2, a/h=30)

	l/h			
a/b	0	0.5	1	2
1	10.7822	5.3763	2.1500	0.6313
1.5	20.7694	10.3644	4.1417	1.2177
2	28.0010	13.9789	5.5856	1.6422

Figure 1 compares the bending values of different nanoplates under sinusoidal load for different material length scale parameters to thickness and length to width ratio. As shown in the picture, the mentioned parameters affect the bending ratio as discussed in "Table 1" . Figure 2 shows the bending contours of a Nth order simply supported nanoplate under the transverse load q. According to the results, the maximum bending value occurs at the midplane point.

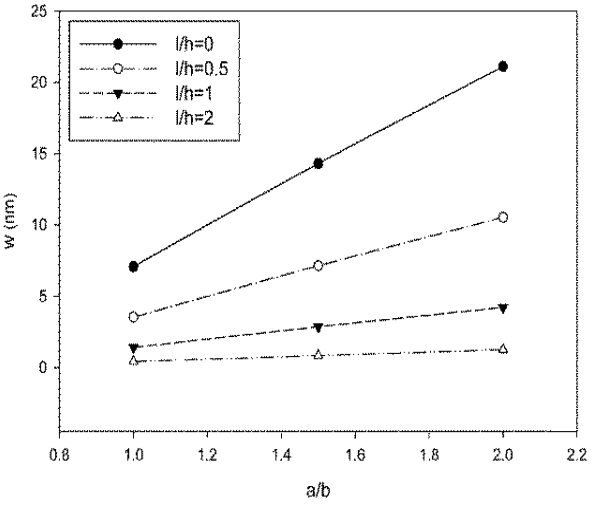

Fig. 1 Comparison of bending values of a Nth order nanoplate under the sinusoidal surface traction for different length to width and length scale parameter to thickness ratios (a/h=30, l/h=1, q=1e-18 N/nm^2).

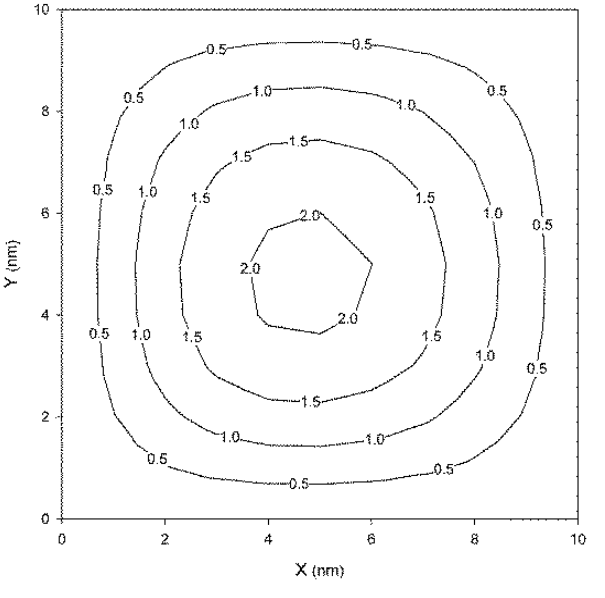

Fig. 2 The bending contours of a Nth order nanoplate (a/h=30, l/h=1, q=1e-18 N/nm^2, a/b=1, n=5).

Table 3 compares the dimensionless bending values of a Nth order nanoplate under the uniform surface traction and sinusoidal load for material length scale to thickness and length to width ratios. As shown in the table, except for the classical theory (I=0), the dimensionless bending values under sinusoidal load were lower than bending values obtained under the uniform surface traction. However, when the material length scale is neglected the bending responses under the two types of load are the same.

Table 3 The comparison of dimensionless bending values of a Nth order nanoplate under uniform surface traction and sinusoidal load for various material length scale to thickness and length to width ratios (n=5, a/h=30, q=1e-18 N/nm^2)

a/b	l/h							
	0		0.5		1		2	
	Uniform load	Sinusoidal load	Uniform load	Sinusoidal load	Uniform load	Sinusoidal load	Uniform load	Sinusoidal load
1	1.00000	1.00000	0.49863	0.49845	0.19918	0.19907	0.05855	0.05851
1.5	1.00000	1.00000	0.499902	0.49872	0.19941	0.19923	0.05863	0.05857
2	1.00000	1.00000	0.49915	0.49885	0.19949	0.19931	0.05865	0.05859

Figure 3 compares the bending values of different nanoplates under sinusoidal load for different material length scale parameters to thickness. As can be seen, the Kirchhoff's nanoplate yielded the lowest values and the third-order nanoplate yielded the highest values for bending.

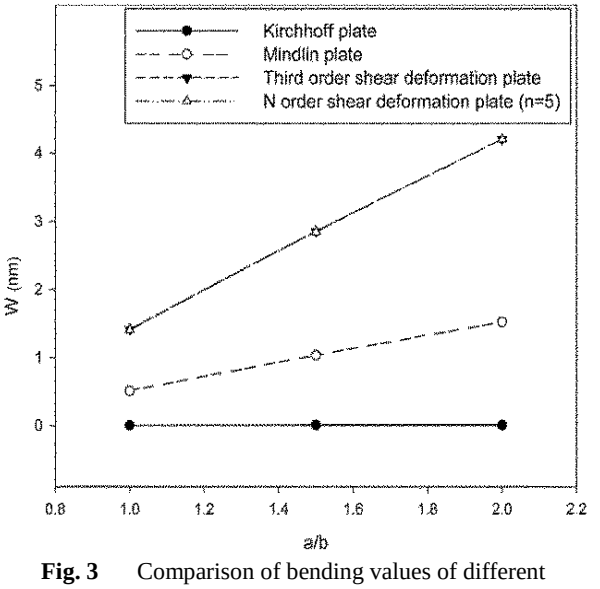

Fig. 3 Comparison of bending values of different nanoplates under the sinusoidal surface traction for different length to width ratios (a/h=30, l/h=1, q=1e-18 N/nm^2).

Figure 4 shows that the critical force value of a Nth order nanoplate under bi-axial loading in the x-y plane, increases due to an increase in the material length scale to thickness and decreases due to an increase in length to width ratio. Figure 5 compares the dimensionless buckling load values of a Nth order nanoplate under the uniform surface traction in the x direction for various material length scale to thickness and length to width ratios. As can be seen, dimensionless buckling load increases due to an increase in the material length scale to thickness and slightly decreases due to an increase in length to width ratio.

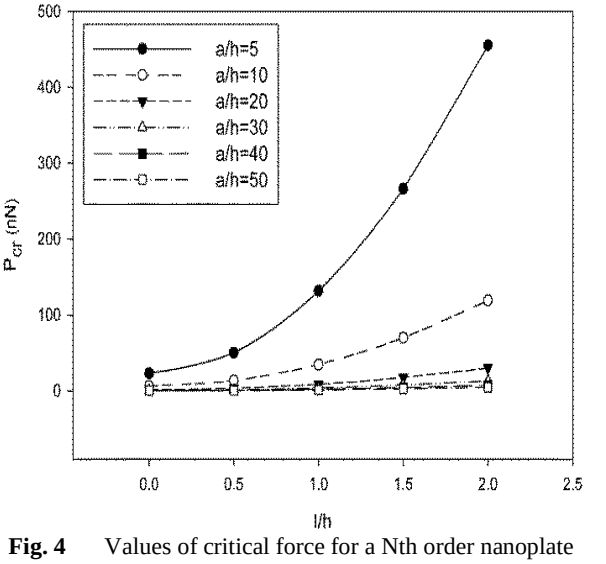

Fig. 4 Values of critical force for a Nth order nanoplate under a bi-axial surface force in x and y directions for material length scale to thickness and length to thickness ratio of the nanoplate (a/b=1, n=5).

Table 4 compares dimensionless buckling load values of different nanoplates under axial and bi-axial loads. As can be seen, the Kirchhoff's nanoplate yielded the lowest values and the Mindlin's nanoplate yielded the highest values for buckling. And also under the bi-axial loading in the x-y plane the plate's responses due to an increase in the material length scale parameter are as follows:

- The dimensionless buckling load of the Mindlin's nanoplate increases.
- The dimensionless buckling load of 3rd and 5th order shear nanoplate slightly decreases.
- The dimensionless buckling load of Kirchhoff's nanoplate remains constant.

Table 4 compares dimensionless buckling load values of 3rd and 5th order nanoplate under axial loading. The results show that the dimensionless buckling load values for the 5th order nanoplate are higher than that of the 3rd order nanoplate.

Table 4 The comparison of dimensionless buckling values for different nanoplates under uniaxial and bi-axial loads for various material length scale to thickness and length to width ratios (n=5, a/h=30, q=1e-18 N/nm^2)

a/h	Kirchhoff plate		Mindlin plate		Third order shear deformation plate		N order shear deformation plate (n=5)	
	Bi-axial buckling	Uniaxial buckling	Bi-axial buckling	Uniaxial buckling	Bi-axial buckling	Uniaxial buckling	Bi-axial buckling	Uni-axial buckling
5	5.0000	5.0000	10.1594	10.1594	5.6521	5.6521	5.6937	5.6937
10	5.0000	5.0000	12.8101	12.8101	5.1723	5.1723	5.1826	5.1826
20	5.0000	5.0000	13.6820	13.6820	5.0437	5.0437	5.0463	5.0463
30	5.0000	5.0000	13.8568	13.8568	5.0195	5.0195	5.0206	5.0206
40	5.0000	5.0000	13.9191	13.9191	5.0110	5.0110	5.0116	5.0116
50	5.0000	5.0000	13.9481	13.9481	5.0070	5.0070	5.0074	5.0074

Table 5 The comparison of dimensionless buckling values of the third and fifth order nanoplates under uniaxial loads for various length to width ratios (n=5, a/h=30, q=1e-18 N/nm^2) (all the quantities for n=0 are 1.00000)

a/h	l/h							
	0.5		1		1.5		2	
	n=3	n=5	n=3	n=5	n=3	n=5	n=3	n=5
5	2.1654	2.18047	5.6521	5.69366	11.4581	11.53596	19.5847	19.71135
10	2.0442	2.04832	5.1723	5.18258	10.3835	10.40186	17.6785	17.70759
20	2.0113	2.01231	5.0437	5.04627	10.0972	10.10167	17.1718	17.17888
30	2.0050	2.00549	5.0195	5.02062	10.0433	10.04529	17.0765	17.07967
40	2.0028	2.00309	5.0110	5.01161	10.0244	10.02549	17.0431	17.04485
50	2.0018	2.00198	5.0070	5.00743	10.0156	10.01632	17.0276	17.02871

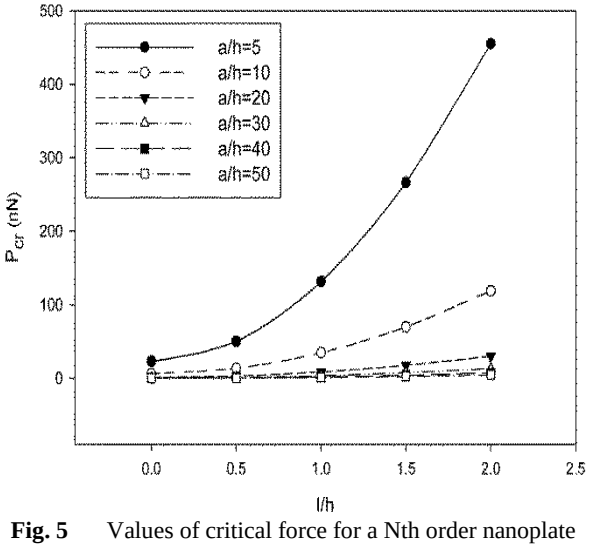

Fig. 5 Values of critical force for a Nth order nanoplate under a uniaxial surface force in x direction for material length scale to thickness and length to thickness ratio of the nanoplate (a/b=1, n=5).

11 CONCLUSIONS

In this study, the bending and buckling of a Nth order nanoplate were investigated using the modified couple stress theory. As observed in the tables and figures, the nth order nanoplate's bending rate under uniform surface traction load decreases with an increase in length scale parameter to thickness ratio of the nanoplate, but, it increases with an increase in the aspect ratio of the nanoplate. Furthermore, the dimensionless bending values under sinusoidal and uniform surface tractions were compared and it was found that when the material length scale is neglected, the bending value is the same for both the loading but otherwise the bending value is always lower under the sinusoidal loading.

The buckling analysis under uniaxial loading showed that the critical force value increases due to an increase in material length scale parameter to thickness ratio but slightly decreases due to an increase in the length to thickness ratio of the nanoplate. It was also found that the critical force value of a 5th order nanoplate is higher than that of 3rd order one.

REFERENCES

[1] Daghigh, H., Daghigh, V., Milani, A., Tannant, D., Lacy, T. E., and Reddy, J. N, Nonlocal Bending and Buckling of Agglomerated CNT-Reinforced Composite Nanoplates, Composites Part B: Engineering, Vol. 183, 2020, 107716. DOI:10.1016/j.compositesb.2019.107716.

[2] Daikh, A. A., Houari, M. S. A., and Eltaher, M. A, A Novel Nonlocal Strain Gradient Quasi-3D Bending Analysis of Sigmoid Functionally Graded Sandwich Nanoplates. Composite Structures, In Press, 2020, 113347. DOI:10.1016/j.compstruct.2020.113347.

[3] Ruocco, E., & Reddy, J. N, Buckling analysis of elastic–plastic nanoplates resting on a Winkler–Pasternak foundation based on nonlocal third-order plate theory. International Journal of Non-Linear Mechanics, Vol. 121, 2020, 103453, DOI:10.1016/j.ijnonlinmec.2020.103453.

[4] Banh Thien, T., Dang Trung, H., Le Anh, L., Ho Huu, V., and Nguyen Thoi, T., Buckling Analysis of Non-Uniform Thickness Nanoplates in an Elastic Medium Using the Isogeometric Analysis. Composite Structures, Vol. 162, 2017, pp. 182-193. DOI:10.1016/j.compstruct.2016.11.092.

[5] Yang, F., Chong, A. C. M., Lam, D. C. C., and Tong, P., Couple Stress Based Strain Gradient Theory for Elasticity, Int. J. Solids Struct, No. 39, 2002, pp. 2731–2743, DOI: 10.1016/S0020-7683(02)00152-X.

[6] Toupin, R. A., Elastic Materials with Couple Stresses, Arch. Rational Mech. Anal, No. 11, 1962, pp. 385–414.

[7] Mindlin, R. D., Tiersten, H. F., Effects of Couple-Stresses in Linear Elasticity, Arch. Rational Mech. Anal, No. 11,1962, pp. 415–448.

[8] Koiter, W. T., Couple Stresses in The Theory of Elasticity, I and II. Proc. K. Ned. Akad. Wet. (B), No. 67, 1964, pp. 17–44.

[9] Mindlin, R. D., Micro-Structure in Linear Elasticity, Arch. Rational Mech. Anal, No. 16, 1964, pp. 51–78.

[10] Tsiatas, G. C., A New Kirchhoff Model Based On a Modified Couple Stress Theory, International Journal of solids and structures, No. 46, 2009, pp. 2757-2764. DOI: 10.1016/j.ijsolstr.2009.03.004.

[11] Wang, B., Zhou, S., Zhao, J., and Chen, X., Asize-Dependent Kirchhoff Micro-Plate Model Based On Strain Gradient Elasticity Theory, European Journal of Mechanics A/Solids, No. 30, 2011, pp. 517-524. DOI: 10.1016/j.euromechsol.2011.04.001.

[12] Farajpour, A., Shahidi, A. R., Mohammadi, M., and Mahzoon, M., Buckling of Orthotropic Micro/Nanoscale Plates Under Linearly Varying In-Plane Load Via Nonlocal Continuum Mechanics, Composite Structures, No. 94, 2012, pp. 1605-1615. DOI:10.1016/j.compstruct.2011.12.032.

[13] Tai, T., Ho Choi, D., Size-Dependent Functionally Graded Kirchhoff and Mindlin Plate Theory Based On a Modified Couple Stress Theory, Composite Structures, No. 95, 2013, pp.142-153. DOI: 10.1016/j.compstruct.2012.08.023.

[14] Akgoz, B., Civalek, O., Free Vibration Analysis for Single –Layered Graphene Sheets in an Elastic Matrix Via Modified Couple Stress Theory, Materials and Design, No. 42, 2012, pp. 164-171. DOI: 10.1016/j.matdes.2012.06.002

[15] Roque, C. M. C., Ferreira, A. J. M., and Reddy, J. N., Analysis of Mindlin Micro Plates with A Modified Couple Stress Theory and Meshlessmethod, Applied Mathematical Modeling, No. 37, 2013, pp. 4626-4633. DOI: 10.1016/j.apm.2012.09.063.

[16] Thai, H. T., Kim, S. E., A Size-Dependent Functionally Graded Reddy Plate Model Based On a Modified Couple Stress Theory, Composites Part B: Engineering, Vol. 45, 2013, pp. 1636-1645. DOI:10.1016/j.compositesb.2012.09.065.

[17] Lou, J., He, L., and Du, J., A Unified Higher Order Plate Theory for Functionally Graded Microplates Based On the Modified Couple Stress Theory, Composite Structures, No. 133, 2015, pp. 1036-1047. DOI: 10.1016/j.compstruct.2015.08.009.

[18] Xiang, S., Kang, G. w., A Nth-Order Shear Deformation Theory for The Bending Analysis On the Functionally Graded Plates, European Journal of Mechanics - A/Solids, No. 37, 2013, pp. 336-343. DOI: 10.1016/j.euromechsol.2012.08.005.